

## Κρουστική διέγερση ράβδου και ακουστικοποίηση στο πεδίο του χρόνου

Σπύρος Κουζούπης  
skouzo@hmu.gr

Χρήστος Παναγιωτόπουλος  
pchr@civil.auth.gr

Άγγελος Κόντος-Πανταζής  
Kontos\_A@hotmail.com

Ελληνικό Μεσογειακό Πανεπιστήμιο,  
Τμήμα Μουσικής Τεχνολογίας και Ακουστικής, Ρέθυμνο 74133, Κρήτη.

### ΠΕΡΙΛΗΨΗ

Η μοντελοποίηση στο πεδίο του χρόνου του πλήκτρου ενός ιδιόφωνου μουσικού οργάνου, όπως του βιμπράφωνα ή της μαρίμπας, το οποίο διεγείρεται από μία μπαγκέτα με σφαιρική κεφαλή, πραγματοποιείται εφαρμόζοντας την μέθοδο των πεπερασμένων στοιχείων. Η μπάρα του μουσικού οργάνου μοντελοποιείται ως μία δοκός τύπου Euler-Bernoulli, αφού έχει προηγηθεί βελτιστοποίηση του προφίλ της, ώστε να επιτευχθούν από μουσικής πλευράς κατάλληλοι λόγοι, μεταξύ των τριών χαμηλότερων ιδιοσυχνοτήτων της. Δεδομένου ότι τα μουσικά όργανα παίζονται συνήθως σε κλειστούς χώρους, αναζητείται ένα ρεαλιστικό ακουστικό αποτέλεσμα λαμβάνοντας υπόψη την επίδραση του περιβάλλοντος χώρου. Αυτό περιλαμβάνει την δονητικο-ακουστική αλληλεπίδραση της ράβδου με το περιβάλλον. Το δυναμικό πρόβλημα αρχίζει να λαμβάνει χώρα από τη στιγμή που κρούεται η δοκός, για αυτό παρέχεται λεπτομερής ανάλυση της επίδρασης κατά την αρχική φάση του δυναμικού προβλήματος. Ο ήχος που προκύπτει από μία μόνο μπάρα καταγράφεται από εικονικούς αισθητήρες, οι οποίοι τοποθετούνται σε διάφορα σημεία εντός ενός κλειστού ή ενός ανοικτού χώρου. Επιπροσθέτως, εξετάζεται και το σενάριο όπου ένας διδιάστατος σωλήνας τοποθετείται κάτω από το πλήκτρο (που είναι ένας κοινός τρόπος για τη βελτίωση του ήχου σε πραγματικά μουσικά όργανα). Πραγματοποιούνται ακουστικοποιήσεις σε πολλαπλές τοποθεσίες εντός του χώρου και με διάφορους συνδυασμούς υλικών της μπάρας και της κεφαλής της μπαγκέτας. Αν και το βασικό δονητικο-ακουστικό πρόβλημα εξετάζεται σε δύο διαστάσεις, η ποιοτική αξιολόγηση των ληφθέντων σημάτων μέσω των εικονικών αισθητήρων, είναι αρκετά ικανοποιητική, όπως προκύπτει από τις δοκιμές ακρόασης.

# Beam auralization in the time domain using the finite element method

## ABSTRACT

*Time-domain modeling of a mallet percussive musical instrument, like an aluminum vibraphone or a wooden marimba bar, struck by a spherical mallet head, is conducted using the finite element method. The bar is modeled as an Euler-Bernoulli beam. Eigenvalue optimization previously led to a non-uniform bar profile with the three lowest eigenfrequencies in proper musical ratios. Given that musical instruments are typically played in enclosed spaces, a realistic acoustic profile is sought by considering the impact of the surrounding room. This involves the vibro-acoustic interaction of the bar with the surrounding air. The dynamic problem is addressed as the beam is struck by a rounded mallet head. A detailed analysis of the impact during the initial phase of the dynamic issue is also provided. The resulting sound from a single bar is captured by virtual sensors positioned at various points within the room or in open space. Additionally, scenarios where a 2D tube is placed under the bar (a common method for sound sustain in real musical instruments) are explored. Auralizations are carried out at multiple locations within the room and with various combinations of bar and mallet head materials. While the primary vibro-acoustic problem is examined in 2D, qualitative assessment of the obtained sensor signals, via listening tests, reveals satisfactory outcomes.*

## 1 Introduction

Mallet percussion instruments are classified as tuned idiophones, producing sound through the vibration of their struck sound bars. When the mallet strikes the sound bar, it activates primarily the vertical bending modes, with the eigenfrequencies of these modes corresponding to the predominant partials of the emitted sound. Because sound bars are inherently inefficient as radiators, many instruments incorporate cavity resonators to amplify the sound projection.

The vertical bending modes of sound bars are meticulously adjusted to achieve certain frequency ratios by incorporating specific undercuts, as uniform cross-section bars typically produce nonharmonic eigenfrequencies. The tuning process of marimba and xylophone bars underwent thorough examination by Bork [1], delving into several practical considerations. Orduña-Bustamente [2] and Petrolito and Legge [3] developed numerical techniques to optimize the undercuts for attaining desired harmonic ratios among the partials. Recent studies by Beaton and Scavone delved into iterative and genetic algorithms for optimization purposes [4].

Chaigne and Doutaut [5] introduced numerical simulations of xylophone bars employing a one-dimensional finite difference method, which also scrutinized the nonlinear interaction between the mallet and the sound bar through experiments and simulations. Doutaut and colleagues [6] expanded the model by incorporating a tubular resonator, considering it as a unidimensional system. They noted the negligible impact of the resonator's back-coupling effect on the bar, a characteristic specific to xylophone bars in higher frequency ranges, cautioning against generalizing this to all mallet percussion instruments. Henrique and Antunes [7] presented a modal simulation of sound bar vibrations, accounting for nonlinear interaction phenomena but overlooking acoustical radiation. Present authors have also dealt primarily with the profile shape optimization of the bars, [8, 9, 10].

The development of a physics-based numerical model for sound production in mallet percussion instruments poses several challenges. Addressing sound radiation in open or semi-open spaces necessitates a model capable of handling unbounded domains. Moreover, the nonlinear interaction between the mallet and sound bar complicates frequency domain solutions. This paper explores a broader examination of collision modeling in musical instruments and introduces a finite element (FE) method to address the mentioned challenges, demonstrating its efficacy in the time domain through various case studies involving different materials for the bar and the mallet, as well as different striking velocities and positions.

Mallets for the xylophone are typically made of polyester, rubber, or wood. Articulation is crucial in mallet selection. The marimba, glockenspiel, and vibraphone have resonance influenced by mallet choice, while the xylophone behaves differently. It has a short staccato response. The mallet's hardness alters the initial attack of a note. Harder mallets create a brighter, louder tone,

while softer ones like rubber produce a warmer, rounder tone. Wooden mallets are also a solid option. The size of the mallet's head affects articulation and dynamics. A smaller ball produces a thinner tone, while a larger one offers a fuller response from the bar. This principle applies to all mallet instruments.

## 2 Spatiotemporal consideration for the excitation of the instrument's bar

Percussion mallets are made from a diverse range of materials. In the following analysis, we will calculate various physical attributes, considering both standard and extreme scenarios, such as using an exceptionally hard or soft mallet head to strike either a hard (metal) or softer (wooden) bar. We will focus on three mallet materials: rubber, wood, and aluminum, and two bar materials: wood and aluminum. Notably, the effective mass of the mallets is approximately 20% higher than the actual mass of the mallet head, as demonstrated in some experiments [11].

Utilizing findings from contact theory as proposed by Landau [12], the Hertzian stiffness coefficient  $K$  can be approximated by considering two elastic spheres of distinct materials in contact (without accounting for any vibration of the spheres). If a spherical mallet head with radius  $R_M$ , Young's modulus  $E_M$ , and Poisson's ratio  $\sigma_M$  undergoes compression denoted by  $\delta$ , then the interaction force  $F$  between the two solids can be expressed as

$$F = K \delta^{3/2} \quad (1)$$

where  $K$  for a flat beam is given by  $K = \sqrt{R_M}/D$ , and the combined flexural rigidity  $D$  depends on the Young's moduli and Poisson's ratios of both the beam  $E_B$ ,  $\sigma_B$  and mallet  $E_M$ ,  $\sigma_M$  as illustrated below:

$$D = \frac{3}{4} \left( \frac{1 - \sigma_B^2}{E_B} + \frac{1 - \sigma_M^2}{E_M} \right) \quad (2)$$

The range of  $K$  values for a 1 cm radius mallet head after considering various mallet-bar material combinations is  $8.9 \times 10^6 - 6.3 \times 10^9 \text{ N m}^{-3/2}$ . The lower value corresponds to a rubber mallet head striking a hard wooden bar, while the higher value corresponds to a brass mallet head striking an aluminum bar. Since mallet heads are typically covered with felt or are threaded, accurately estimating the actual value of  $K$  can be challenging. In [11], the experimentally obtained value of  $K$  is  $1.31 \times 10^9 \text{ N m}^{-3/2}$  for a boxwood head striking a xylophone bar (made of hard wood). Although wooden mallets are not commonly used in xylophone playing, plastic or rubber materials are more prevalent.

$$\mu \dot{\delta}^2 + \frac{4\sqrt{R_M}}{5D} \delta^{5/2} = \mu v_o^2 \quad (3)$$

For an aluminum beam with a mass of  $M_B = 0.429 \text{ kg}$  struck by a wooden (padouk) spherical mallet head of radius  $R_M = 1 \text{ cm}$  and mass  $M_M = 0.0262 \text{ kg}$ , traveling at a velocity of  $v_o = 1 \text{ m/s}$ , the compression evolution  $\delta(t)$  can be determined by solving eq. (3). The interaction time is twice the time taken to reach maximum compression [12, 11]. This assumption holds when the force applied on the beam is symmetrical (in time) around its peak value. However, it is generally valid only for very long beams or when the boundary conditions are identical at both ends and the beam is struck at the midpoint. By integrating eq. (3) up to the maximum displacement we can approximate the interaction time as:

$$\tau = 3.218 \left( \frac{\mu^2}{K^2 v_o} \right)^{1/5} \quad (4)$$

However, based on the solution of eq. (3) and under the assumption of the mentioned symmetry, we can easily derive the maximum compression as follows:

$$\delta_{max} = \left( \frac{5\mu v_o^2}{4K} \right)^{2/5} \quad (5)$$

where  $K$  represents the Hertzian constant defined as  $K = \sqrt{R_M}/D$ . By combining eqs. (5) and (4), we can derive an approximation for the interaction time in terms of  $\delta_{max}$  and  $v_o$ :

$$\tau = 2.943 \frac{\delta_{max}}{v_o} \quad (6)$$

Using eq. (5) and assuming a flat beam, the radius of the contact ‘area’ at the point of maximum force, as well as how the radius changes over time, can be described by the following relationships:

$$r_{max} = \sqrt{\delta_{max} R_M} \quad , \quad r(t) = \sqrt{\delta(t) R_M} \quad (7)$$

Since the contact area was assumed to be circular, the impact width  $\Delta x$  can be determined from the contact radius  $r(t)$  and the deformation  $\delta(t)$  by calculating the length of the circular cord. In our implementation, we maintain  $\Delta x(t)$  at a constant value, set to twice the maximum contact radius  $\Delta x = 2 r_{max}$ . In other simulations involving impacts on musical instruments that we are familiar with, the load is usually either evenly distributed over a particular length [11] or applied at a specific point (node) [13, 14]. It has been assumed [5] that in most cases the size of the contact area has a minimal impact, although this necessitates further examination. When considering the parameters  $\delta_{max}$  and velocity  $v_o$  within specific ranges, the estimated impact width falls within a defined range. In the following, we aim to determine the contact force  $F(t)$  and the deflection of the beam  $w(t)$  when the beam is struck with velocity  $v_o$  by a mallet of mass  $m$  with a spherical head. Assuming the validity of the Hertzian law for elastic bodies, the relative approach  $\delta(t)$  is governed by

$$\delta(t) = \kappa F^{2/3}(t), \quad (8)$$

where  $F(t)$  represents the contact force between the two bodies and  $\kappa$  is the Hertzian constant [12], which relies on the elastic moduli and contact geometries of the bodies involved. The relative approach is defined as the disparity between the displacement  $w_s$  of the striking sphere caused by the force  $F(t)$  and the displacement  $w_o$  of the beam at the contact point, under the assumption that the sphere has mass  $M_s$ .

$$\delta(t) = w_s - w_o \quad (9)$$

Displacement  $w_s$  is given by:

$$w_s = v_o t - \frac{1}{M_s} \int_0^t F(\tau)(t - \tau) d\tau \quad (10)$$

and the relative approach according to eq. (9) becomes,

$$\delta(t) = v_o t - \frac{1}{M_s} \int_0^t F(\tau)(t - \tau) d\tau - w_o(t) \quad (11)$$

The response of the beam to the impulsive force  $F(t)$  must be analyzed as an expansion in the normal modes based on the beam’s boundary conditions and the location of the impacting force. It is represented [15] as:

$$w_o(t) = \sum_m^\infty a_m g_m(x_o) \int_0^t F(\tau) \sin[\alpha_m(t - \tau)] d\tau \quad (12)$$

The constants  $a_m$  and eigenfunctions  $g_m(x)$  are derived from the particular problem at hand while  $\alpha_m$  denote the eigenvalues of the problem. These values can be found by solving a specific beam vibration problem with particular boundary conditions. In the end, all these elements lead to the

subsequent nonlinear second kind Volterra-type integral equation:

$$\begin{aligned} \kappa F^{2/3}(t) = v_o t - \frac{1}{M_s} \int_0^t F(\tau)(t - \tau)d\tau \\ - \sum_m^\infty a_m g_m(x_o) \int_0^t F(\tau) \sin[\alpha_m(t - \tau)]d\tau \end{aligned} \quad (13)$$

After examining the literature on musical instruments, as far as the authors are aware, this specific formulation has not been cited or implemented. The resolution of this equation can be accomplished using numerical and approximate analytical approaches. During an iterative process for solving an equation like this, a trial function is typically selected for the force, and the integrals of the previous equation are calculated numerically to update the force value. However, this can sometimes result in inconsistencies at the trailing edges of the force pulse. To address this issue, we will apply the approach described in [15], where the force is assumed to change linearly during each small time increment  $dt$ . While the specifics of this technique are not reiterated here, we have applied this method to determine the contact force in scenarios involving a round shape (such as a cylinder or sphere) impacting a beam at a specific location.

When confronted with a non-uniform beam possessing an intricate profile, like the one present in an idiophone musical instrument, a similar strategy can be utilized. In this case, the numerically computed eigenmodes act as replacements for their analytical equivalents. For the case of a spherically shaped mallet striking a beam, eq. (13) becomes

$$\kappa F^{2/3}(t) = v_o t - \frac{1}{M_s} P(t) - \sum_m^\infty a_m g_m(x_o) Q(t) \quad (14)$$

where  $P(t) = \int_0^t F(\tau)(t - \tau)d\tau$  and  $Q(t) = \int_0^t F(\tau) \sin[\alpha_m(t - \tau)]d\tau$ . The last expression relies on the eigenvalues of the problem at hand.

In order to clarify the procedure we consider the problem of a sphere striking at point  $x_o$  a simply supported uniform beam (possessing simple eigenfunctions). The equivalent equation to eq. (13) is the following,

$$\begin{aligned} \delta(t) = \kappa F^{2/3}(t) \\ = v_o t - \frac{1}{M_s} \int_0^t F(\tau)(t - \tau)d\tau - \sum_m^\infty \frac{X_m^2(x_o) \int_0^t F(\tau) \sin[\omega_m(t - \tau)]d\tau}{\rho A \omega_m \int_0^L X_m^2 dx} \end{aligned} \quad (15)$$

where  $X_m(x) = \sin(m\pi x/L)$ ,  $\rho$ ,  $A$  and  $\omega_m = \frac{m^2 \pi^2}{L^2} \sqrt{\frac{EI}{\rho A}}$  are the eigenfunctions, the beam material density, the cross section area and the eigenfrequencies respectively.

Characteristic load shapes, estimated with the method mentioned above, are depicted in Fig. 2.1 when an aluminum mallet strikes with three different velocities on an aluminum optimized beam at position  $x = 0.202$ . Load shapes of this kind were utilized in the subsequent analyses.

### 3 Beam profile optimization process

Since we are interested in controlling the natural frequencies (e.g., eigenfrequencies) of idiophone bars, in this work we computed the dynamic characteristics of structural components with both the FEM and the boundary element method (BEM), a procedure developed elsewhere [10]. Our objective, through the application of appropriate boundary conditions, was to establish a robust body design that ensures the second and third modal frequencies of these systems exhibit predetermined relationships with their respective first modal frequencies. In this study, the resonator's shape remained unaltered.

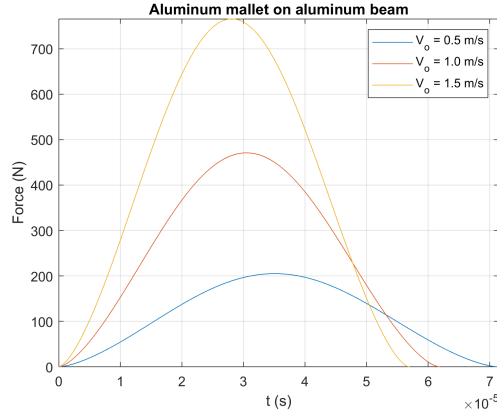


Figure 2.1 Characteristic load shapes utilized in the subsequent analyses.

While conducting work in a complete three-dimensional space is feasible and advantageous, we chose to limit our analysis to one-dimensional models for simplicity. It is widely acknowledged that idiophone bars predominantly operate through bending. Therefore, for the purposes of design and simulation, it is generally acceptable to focus on in-plane bending. After discretizing continuous beam profiles and applying the aforementioned methods to optimize eigenfrequencies in the ratios of (1 : 4 : 9.8), the resultant beam was used in the subsequent analyses.

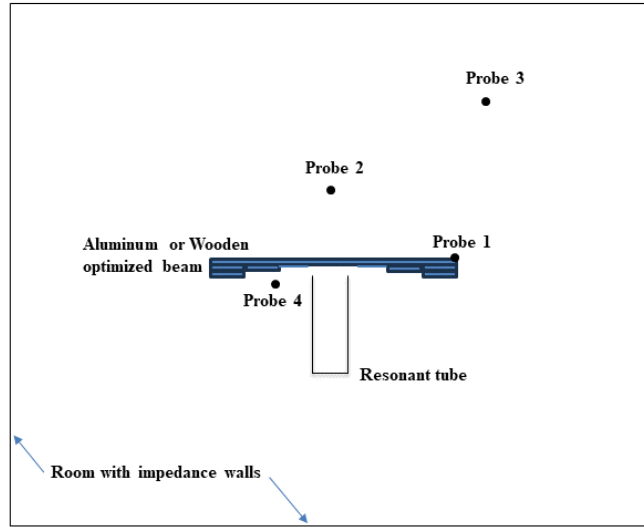


Figure 3.1 Optimized beam in a confined space with a resonator underneath. Note that the bar, the 2D room and the resonant tube are not drawn to scale.

#### 4 Numerical experiments in a 2D domain

The optimized beam was positioned within a rectangular domain with dimensions:  $L_x = 3\text{ m}$  and  $L_y = 3.5\text{ m}$ , as shown in Fig. 3.1. The length of the beam was  $L = 0.5027\text{ m}$ . It consists of 9 segments located at  $x$  positions of 0, 0.0521, 0.1022, 0.1517, 0.2018, 0.3009, 0.3510, 0.4005, 0.4506, 0.5027  $m$  while the respective heights of the steps for an aluminum beam are: 0.010, 0.0075, 0.0066, 0.004, 0.0032  $m$ . The initial step height of the wooden beam (adjusted to match the eigenfrequencies of the aluminum beam) is 0.014547  $m$ , with subsequent segment heights maintaining the same ratios as the aluminum beam. The origin of the axes is at the beam's left end, so probes 1, 2, 3, 4 are positioned at  $(x, y)$  points of  $(L, 0)$ ,  $(L/2, L/4)$ ,  $(L/2 + L_x/4, L_y/3)$ ,  $(0, -0.12\text{ m})$  (Fig. 3.1). The resonant tube of length  $L_t = 1.41\text{ m}$  and width  $W = 0.15\text{ m}$  lies

beneath the beam with a clearance of  $0.03\text{ m}$ . The load application region is slightly off-center between  $0.2018 - 0.2020\text{ m}$ . The wall impedance at the walls is  $0.3 Z_o$ , with  $Z_o$  representing air's characteristic impedance, and Rayleigh damping is applied to the beam.

Numerous numerical experiments were conducted involving various combinations. Two materials for the beam were used: wood and aluminum. The three materials for the mallet head were: aluminum, rubber, and wood and three mallet head velocity values  $v_o$  were used:  $(0.5, 1.0, 1.5\text{ m/s})$ . Experiments also included scenarios with artificial absorbing conditions at boundaries to simulate the open space problem as well as the introduction of a resonant tube to evaluate its effect. Results reported here include only the cases where the resonant tube is present and there is uniform absorption at the boundary walls with typical impedance values. All experiments involving acoustic-structure interaction were conducted in Comsol Multiphysics. 2-D triangle elements with fourth order (quartic) shape functions were utilized in the acoustic domain. In the beam analysis, 2-D finite elements were employed with distinct shape functions for axial and transversal degrees of freedom. Linear shape functions represented axial displacement, whereas cubic shape functions were used for bending. A typical power spectrum of the signal obtained from probe 1, after a rubber mallet head strikes a wooden beam at a velocity of  $1\text{ m/s}$  at  $0.2019\text{ m}$  from the beam's edge, is shown in Fig. 4.1.

The results from the numerical experiments conducted in this study, along with the generated sounds, have been appropriately archived in an online open-access repository. This repository can be accessed via the link provided below<sup>1</sup>.

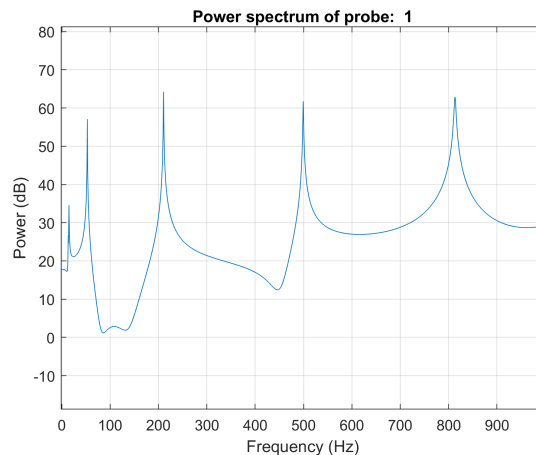


Figure 4.1 *Typical power spectrum of the signal obtained from probe 1, after a rubber mallet head strikes a wooden beam at a velocity of  $1\text{ m/s}$ .*

## 5 Conclusions

In this study, we have successfully conducted time-domain modeling of mallet percussive musical instruments, specifically for aluminum vibraphone and wooden marimba bars, when struck by spherical mallet heads using the finite element method. By modeling the bar as an Euler-Bernoulli beam and optimizing eigenvalues to achieve proper musical ratios, we have obtained a non-uniform bar profile. Considering that musical instruments are often played in enclosed spaces, we further explored the realistic acoustic profile by examining the vibro-acoustic interaction of the bar with the surrounding air. Our analysis of the dynamical problem, particularly during the initial phase of impact, has provided valuable insights. Through the use of virtual sensors placed strategically within the room or open space, we captured the resulting sound from a single bar and explored scenarios involving a 2D tube placed under the bar for sound sustain, a common technique in real musical instruments. The conducted auralizations, recorded at multiple locations within the room and utilizing various combinations of bar and mallet head materials, have

<sup>1</sup><https://gitlab.com/KontosA/helina2024>

contributed to our understanding of the vibro-acoustic problem. While our examination primarily focused on two-dimensional analysis, qualitative assessments of sensor signals through listening tests have yielded satisfactory results. These findings facilitate the transition to three-dimensional implementation and provide opportunities for further research and enhancements in the design and acoustics of mallet percussion instruments, while also paving the way for potential improvements in the excitation aspect of the problem.

## 6 References

- [1] I. Bork, “Practical tuning of xylophone bars and resonators,” *Applied Acoustics*, vol. 46, pp. 103–127, 1995.
- [2] F. Orduña-Bustamante, “Nonuniform beams with harmonically related overtones for use in percussion instruments,” *Journal of the Acoustical Society of America*, vol. 90, pp. 2935–2941, 1991.
- [3] J. Petrolito and K. A. Legge, “Optimal undercuts for the tuning of percussive beams,” *Journal of the Acoustical Society of America*, vol. 102, pp. 2432–2437, 1997.
- [4] D. Beaton and G. P. Scavone, “Optimization of marimba bar geometry by 3D finite element analysis,” 2019.
- [5] A. Chaigne and V. Doutaut, “Numerical simulations of xylophones. I. time-domain modeling of the vibrating bars,” *Journal of the Acoustical Society of America*, vol. 101, pp. 539–557, 1997.
- [6] V. Doutaut, D. Matignon, and A. Chaigne, “Numerical simulations of xylophones. II. time-domain modeling of the resonator and of the radiated sound pressure,” *Journal of the Acoustical Society of America*, vol. 104, pp. 1633–1647, 1998.
- [7] L. Henrique and J. Antunes, “Optimal design and physical modelling of mallet percussion instruments,” *Acta Acustica*, vol. 89(6), pp. 948–963, 2003.
- [8] S. Kouzoupis, “Theoretical approach on the use of beams as musical idiophones,” in *Proceedings of the 9th HELINA Conference, (Hellenic Institute of Acoustics)*, University of Patras, 2018.
- [9] X. Παναγιωτόπουλος, Σ. Κουζούπης, Α. Κρυονερίτης και Α. Κόντος-Πανταζής, “Βελτιστοποίηση σχήματος για τον σχεδιασμό ιδιοφώνων και πειραματική διερεύνηση,” in *ΕΛ.ΙΝ.Α, Ακουστική 2022, Θεσσαλονίκη 14-17 Οκτωβρίου*, 2022.
- [10] C. G. Panagiotopoulos and S. Kouzoupis, “Tuning of idiophones using shape optimization on finite and boundary element 1D models,” *Applied Acoustics*, vol. 217, p. 109850, 2024.
- [11] A. Chaigne and V. Doutaut, “Numerical simulations of xylophones. i. time-domain modeling of the vibrating bars,” *The Journal of the Acoustical Society of America*, vol. 101, no. 1, pp. 539–557, 1997.
- [12] L. Landau and E. Lifchitz, *Théorie de l'élasticité*. Mir, 1967.
- [13] P. Rucz, M. Á. Ulveczki, J. Angster, and A. Miklós, “Simulation of mallet percussion instruments by a coupled modal vibroacoustic finite element model,” *The Journal of the Acoustical Society of America*, vol. 149, no. 5, pp. 3200–3212, 2021.
- [14] L. L. Henrique and J. Antunes, “Optimal design and physical modelling of mallet percussion instruments,” *Acta Acustica united with Acustica*, vol. 89, no. 6, pp. 948–963, 2003.
- [15] G. Evans, B. Jones, A. McMillan, and M. Darby, “A new numerical method for the calculation of impact forces,” *Journal of Physics D: Applied Physics*, vol. 24, no. 6, p. 854, 1991.